Weihua Cai
Hydronics Laboratory,
Department of Aerospace and Mechanical Engineering,
University of Notre Dame,
Notre Dame, IN 46556

Walfre Franco
Beckman Laser Institute and Medical Clinic,
University of California,
Irvine, CA 92612

Gregor Arimany
Department of Civil Engineering and Geological Sciences,
University of Notre Dame,
Notre Dame, IN 46556

Mihir Sen

K. T. Yang

Rodney L. McClain

Hydronics Laboratory,
Department of Aerospace and Mechanical Engineering,
University of Notre Dame,
Notre Dame, IN 46556

Interaction Between Secondaries in a Thermal-Hydraulic Network

The design of one secondary loop of a complex network often neglects the effect that its operation has on the others. The present is a study of hydrodynamic and thermal interaction between secondaries in a thermal-hydraulic network as the system goes from one steady state to another. Experimental results are related to those derived from a mathematical model. The network consists of a primary and three secondary loops. There is a water-to-water heat exchanger on each secondary, with the cooling coming from the primary and the heating from a separate loop. A step change is introduced by manually actuating a valve in one of the secondaries, resulting in changes in the other loops also. The response time of the temperature is found to be an order of magnitude higher than that of the flow rate, which is again an order of magnitude higher than the pressure difference. The steady-state results show that there is significant interaction, and that it is dependent on the initial operating condition. The hydrodynamic and thermal responses are found to be very different. [DOI: 10.1115/1.2363411]

1 Introduction

In general, a thermal-hydraulic network consists of a heating or cooling plant, energy conversion components, boilers and condensers, a complex layout of piping, and pumps that drive water or some other fluid to heat exchangers for end-users that may be located at some distance. Such networks form a fundamental part of climate control systems in buildings, and are also used in the process and energy generation industries. Components such as heat exchangers, pipes, pumps, and turbines have been well studied, but when various components are put together to constitute a complex network, the performance of the whole system is different from that of its individual components since each is affected by others in its neighborhood.

There has been work reported on network performance affected by the behavior of key components or subsystems. For example, a common problem in chilled-water plants is that the temperature differential is frequently not at its design value due to improper thermal loads [1]. Even small changes in piping arrangements can significantly affect the performance of the system preventing it from achieving optimum operating conditions [2,3]; some practical solutions have been suggested to achieve high performance in this case [4–6]. Simulation of flows and temperatures in a thermal-hydraulic network, especially in a large-scale network, is often done by assuming a quasidynamic approximation between flow and temperature [7]; that is, the flow is computed independently from the temperature distribution, and the temperature is computed by assuming constant flow in the whole network.

The proper operation of subsystems is vital to the overall energy efficiency and directly affects the performance of the entire network. Poorly-designed subsystems can decrease the temperature differentials in chillers [4] which do not work efficiently when the network does not perform at design conditions because of flow and thermal interactions [8]. The supply and return water temperatures in the circulation network also greatly affect the primary energy consumption [9]. The design of one subsystem is often carried out by neglecting its effect on the others by, for example, optimizing it in terms of its own operation [10]. Thus a control system for a specific component may be designed on the assumption that the rest of the system is unaffected by its actuation. The functioning of an independent controller in a secondary, however, may negatively affect controllers in the others because of flow and thermal interactions [8,11]. An important point of concern with thermal-hydraulic networks is the resulting unbalanced distribution of heat and flow to the end-users. Accommodations are sometimes made by valve adjustments [12], system retrofit [12,13] and resizing of control valves [4] to balance the thermal and flow distribution.

To design systems which run more efficiently and to optimize control and operate complex systems, it is necessary to investigate the interactions that occur within the different components of the systems. Finding the steady-state interaction between the loops is the purpose of this study. Because of the difficulties associated with the determination of the parameters in mathematical models alone, it was decided to work with experiments in addition to modeling. The objective of the present work is to study the interaction that occurs in a specific thermal-hydraulic network from

Contributed by the Dynamic Systems, Measurement, and Control Division of ASME for publication in the JOURNAL OF DYNAMIC SYSTEMS, MEASUREMENT, AND CONTROL. Manuscript received July 21, 2005; final manuscript received January 16, 2006. Assoc. Editor: Noah Manring.

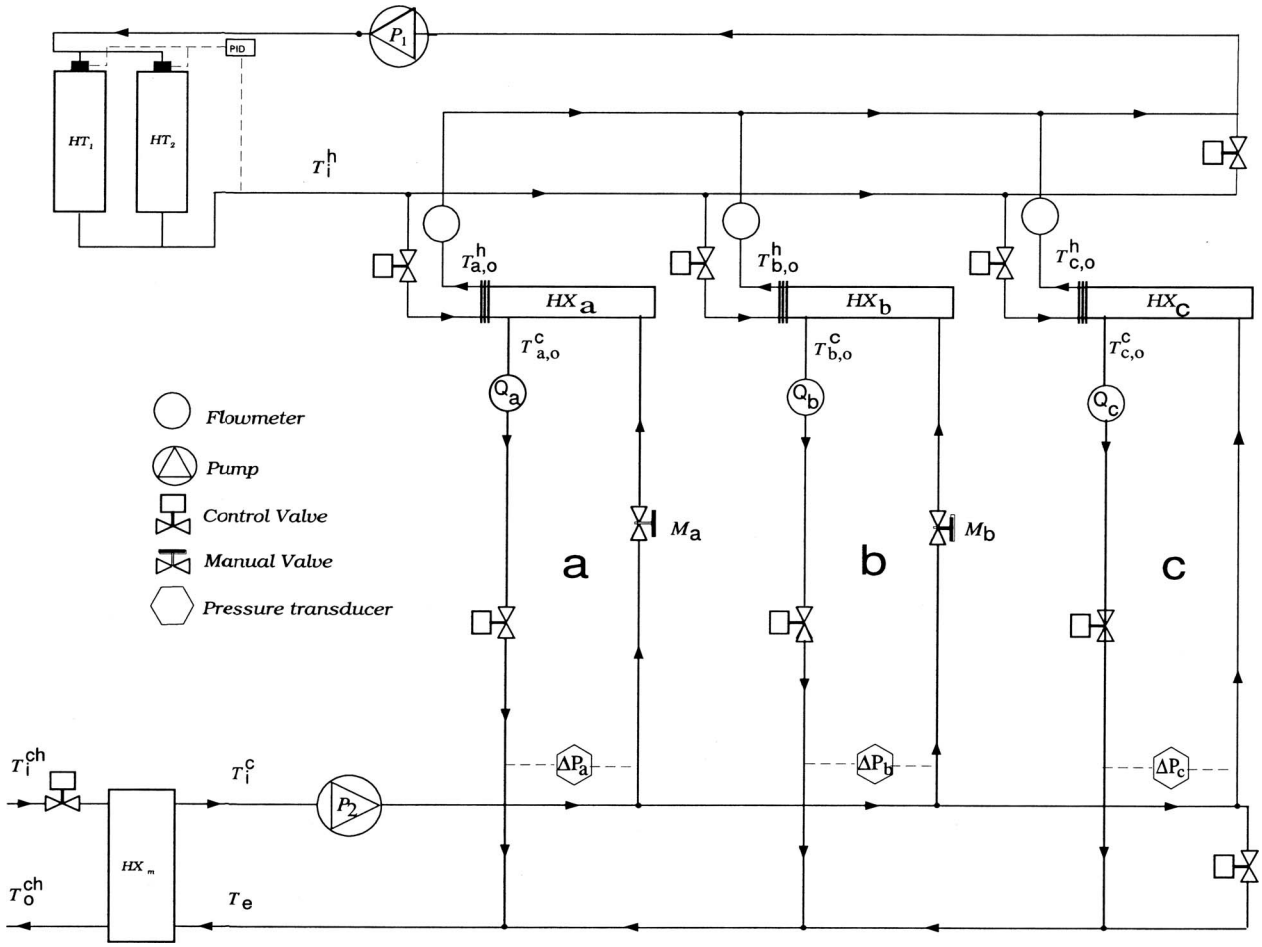

Fig. 1 Schematic of experimental facility. a, b, and c are secondary loops

both points of view. For the purpose of experiments, a cold-water network was constructed with one primary and three secondary loops. Each secondary has a heat exchanger which exchanges heat with a separate hot-water loop. A step change in one secondary loop is introduced by the actuation of a valve, and the hydrodynamic and thermal response of the others is observed. The mathematical model is one dimensional.

2 Experimental Facility and Procedure

A diagram of the experimental facility is shown in Fig. 1 [8]. There is a cold-water primary circuit that feeds several cold-water secondary loops. A 1.5 HP, variable-speed pump P2 (Bell & Gossett series 90, 15 gpm @ 60 ft of water) drives the water. A compact, brazed plate heat exchanger (Bell & Gossett, BP415-50) placed in this circuit uses chilled water provided by the building for cooling purposes. The approximate water-flow distance through the primary and one secondary is 18 m, which gives an idea of the size of the network.

Although a minimum of two secondaries is needed to observe the interaction, it was decided to have three in order to be able to examine the effect of distance between the loop where the step change is made and that where the interaction is observed. In the figure, the three secondaries are marked as **a**, **b**, and **c**. Each secondary has a four-pass water-to-water shell and tube heat exchanger (Bell & Gossett, 308-4S). There is a PID-controlled two-way bronze valve (Johnson Controls, VG7000 Series) on each secondary mounted with a pneumatic valve actuator (Johnson Controls, V-3000-8011). The actuator responds to an electropneumatic transducer (Johnson Controls, EP-8000-2) that converts the voltage signal from a controller into a pneumatic output pressure signal to set the operating flow rate. The controllers are initially applied to set identical initial flow rates in the secondary loops, but are subsequently turned off. There are two brass ball valves M_a and M_b (Watts Regulator, FBV-3), located on loops **a** and **b**, respectively. Manual changes in valve positions are produced by striking quickly with a hammer.

The other sides of the heat exchangers lie on a hot-water circuit. Hot water is generated by a 6 kW heater HT1 (Chromalox, NWHMT-03-006P-E1) and a 15 kW heater HT2 (Chromalox, NWH-31525XX). The water temperatures are maintained at 37.8°C by a single PID controller (RKC Instruments, REX-F400). The water is driven by a 3/4 HP, 60 Hz pump P1 (TEEL, 1P833), and the flow rate at each heat exchanger can be set by a PID-controlled two-way valve.

Data acquisition, processing and setpoint control are carried out by a PC with National Instruments boards (PCI-6033E, PCI-6704, and PCIMIO-16E-4) and LabVIEW software. The temperature of the water is measured by type J ungrounded thermocouples shielded from the water by a thermocouple probe with a time constant of 0.55 s. Water flows are measured by turbine meters (Omega, FTB-4607 on the main cooling loop and FTB-4605 everywhere else), the responses of which are not fast enough for transients to be measured. Pressure differences are measured through pressure transducers (Omega, PX26-030DV) with a response time of 0.001 s. The locations of the measuring points are indicated in Fig. 1.

In the experiment, the dynamic and static responses of the system to step changes in valve setting in one of the secondary loops is determined. Since the secondary loops are in parallel with the primary, they can all be set to operate at identical conditions be-

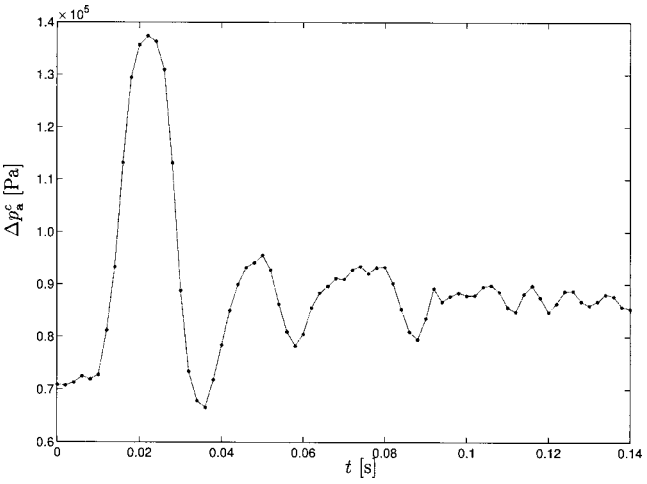

Fig. 2 Pressure wave in loop a

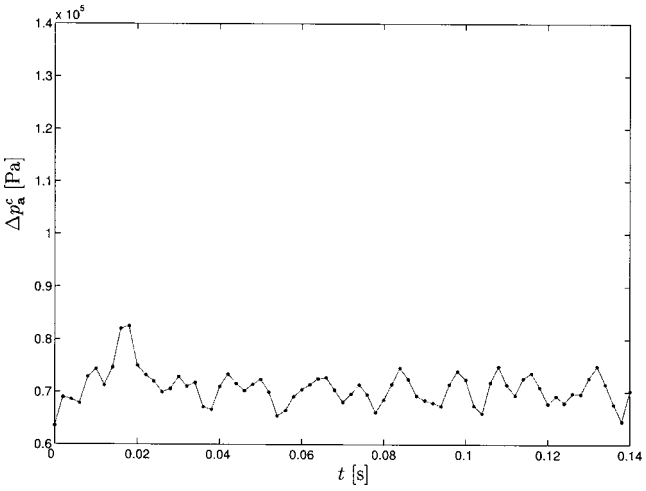

Fig. 3 Transient pressure difference in loop a

fore the step change is introduced. For this purpose the control valves on the heating side of the secondary loops are set using separate PID controllers to maintain the same initial hot-water flow rate, $Q_{\text{set}}^h = 158$ ml/s, in all three secondaries. In the same way, the control valves on the cooling side are also set using separate controllers to maintain the same initial cold-water flow rate Q_{set}^c. After a steady state has been reached, the controllers on both cooling and heating sides are switched off, so that without actuation the valve positions do not change. At this point the three secondary loops are operating at the same hydraulic and thermal conditions.

To understand the pressure response of the system, a preliminary test was made of natural pressure wave oscillations to a severe disturbance. This was created by a large change in valve position under flow conditions. The frequency of these oscillations depends on the properties of water and the elasticity of the pipe. A typical pressure wave is shown in Fig. 2, with the period of the oscillations being about 0.027 s.

A series of step changes is then introduced in a manual valve on the cooling sides of either loop **a** or **b**, which we will call the *actuating* loop. Each change is quick enough to be considered as a step change in comparison to the other time scales in the system. The response of the other two loops, to be called *responding* loops, is determined until a steady state is reached, after which another step change in valve position is effected. This results in a series of valve step changes for a given Q_{set}^c. The measurements are carried out for $Q_{\text{set}}^c = 189$, 127, and 63 ml/s. Two types of responses are studied. The transient response allows us to understand the thermal-hydraulic network as a complex dynamical system. The steady state is that found after the slowest transient has died down.

3 Transient Response

3.1 Flow-Rate Calculation. Since direct measurement was not possible, the transient flow rate is calculated from pressure-difference information. This indirect method provides an insight on the time scale of the flow rate response. We write the one-dimensional momentum equation for flow in a secondary loop, $Q(t)$, as

$$\beta \frac{dQ}{dt} + \alpha Q^n = \Delta p(t) \tag{1}$$

where

$$\beta = \frac{4\rho L}{\pi D^2} \tag{2}$$

D is the pipe diameter, ρ is the fluid density, and L is the pipe length. In Eq. (1) the three terms from the left are inertia, frictional, and pressure forces, respectively. α is a loss coefficient which is due to a combination of the wall-shear stress and losses due to various fittings such as valves, elbows, and tees. The step change occurs at $t=0$. Since all the other contributions to the loss coefficient are the same before and after the step change, there is a change in α in the actuating loop due to the manual valve change. The before and after values of α can be determined from the corresponding steady-state form of Eq. (1), $\alpha = \Delta p / Q^n$. Once the step function $\alpha(t)$ has been found, Eq. (1) can be solved numerically to determine $Q(t)$. Since the exponent n varies between 1 for laminar and 2 for high-Reynolds number flows, unless otherwise stated the calculations are done for the two extremes of n to determine a range within which the flow rate $Q(t)$ must lie.

3.2 Response Times. It is desirable to know the speed of response of the network with respect to each of the three variables: temperature, pressure difference, and flow rate. As a typical result, we will show those for a small valve step change in loop **a**. The pressure difference in the same loop, Δp_a^c, is shown in Fig. 3. There is an overshoot of the pressure difference because of the rapid change of the manual valve setting. The duration of the overshoot is of the same order of the period of a pressure wave within the system. Since the magnitude of the valve change is much smaller than that in Fig. 2, not many periods can be observed before the signal is overcome by noise. The transient pressure time is also affected by the speed with which the valve is closed [14]. The temperature at the outlet of the heat exchanger $\text{HX}_{\mathbf{a}}$ is shown in Fig. 4. The signal has been smoothed with a fifth order Savitzky-Golay FIR filter [15] to eliminate the noise; the rms of the noise is also indicated. Flow rates $Q_{\mathbf{a}}$ and $Q_{\mathbf{b}}$ in loops **a** and **b**, respectively, are shown in Fig. 5.

We can define the response time for a system variable as the approximate time required for it to go from its initial to its final value. The three figures show that the response times of the pressure difference, flow rate, and temperature are approximately of the order of 0.01, 0.1, and 1 s, respectively. Quantitative values are shown in Table 1, where the results of three different runs for $Q_{\text{set}}^c = 189$ ml/s are shown. In each run, because of the speed of the pressure wave in the system, the pressure difference throughout the network is the quickest to respond. The pressure change induces a flow-rate change which is resisted by the fluid inertia and wall-shear stress, so that the response in flow rate is slower.

Table 1 Response times for pressure difference, temperatures, and flow rates for three different runs

Variable	Time (s)	Time (s)	Time (s)
$\Delta p_{\mathbf{a}}$	0.01	0.03	0.02
$T^c_{\mathbf{a},o}$	5.17	5.26	7.33
$T^h_{\mathbf{a},o}$	4.02	3.66	4.56
$T^c_{\mathbf{b},o}$	4.17	2.16	3.69
$T^h_{\mathbf{b},o}$	3.71	1.62	3.09
$Q_{\mathbf{a}}$	0.26–0.36	0.15–0.31	0.13–0.19
$Q_{\mathbf{b}}$	0.09–0.12	0.06–0.09	0.10–0.39

The temperature response is slower still because of the mass of fluid and heat exchanger that has to be heated or cooled.

4 Steady-State Hydrodynamic Response

In this section the pressure and flow rate interaction will be presented. The results are shown in a series of graphs, the symbols for which are indicated in Table 2. Interest is principally on the cooling side of the heat exchangers, and unless otherwise stated all information presented will be from that side.

4.1 Experiment. Figures 6 and 7 show the effect of valve adjustment on the actuating loop. The abscissa is the relative change of flow rate in the actuating loop; the ordinate is the relative change of pressure differences along the secondary loops or the relative change of flow rates in the responding loops. As shown in the figures, closing the valve in the actuating loop results in a decrease of flow in that loop but an increase of pressure differences along secondary loops and flow rates in the responding loops. Figures 6 and 7 both have three groups of lines with different slopes that correspond to three different initial setting of the flow rate Q^c_{set}. The larger the Q^c_{set}, the steeper the slope of the lines and, therefore, the stronger the interaction among the secondary loops. In addition, there is little difference in the pressure drops in the three secondaries, no matter if the actuation takes place in loop **a** or **b**. This means that for this particular network, being relatively small, the distance between the actuating and responding loops does not affect the response results very much.

4.2 Model. A mathematical model can provide physical insight on how the flow is distributed among the secondary loops. Figure 8 is a simplified schematic of the cold-water loops. According to the measurements shown in Table 3, the pressure drops in the short stretches *ab*, *bc*, *cd*, *ef*, *fg*, and *gh* are small compared

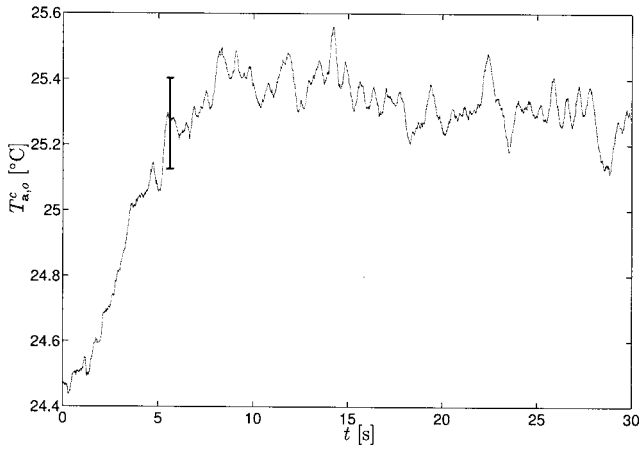

Fig. 4 Transient outlet temperature on the cooling side of loop a. Bar indicates rms difference between raw and smoothed signal.

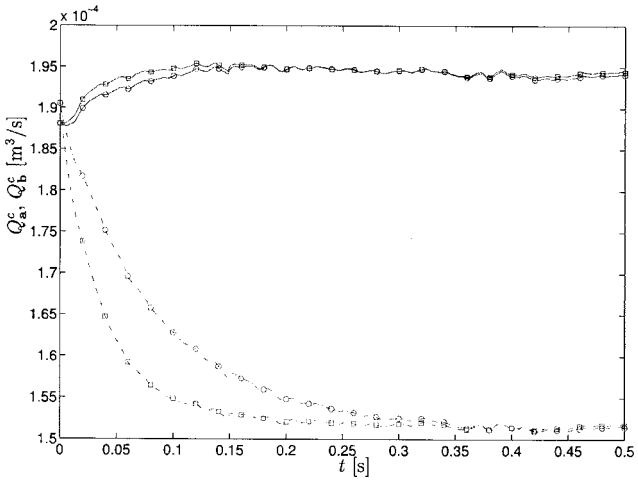

Fig. 5 Transient flow rates in loop a and b; -○- *n*=1, -□- *n*=2; dashed-dotted line: loop a; solid line: loop b

to those in *ae*, *bf*, *cg* or *dh*. Thus we can assume that the pressure drops $\Delta p_{ae}=\Delta p_{bf}=\Delta p_{cg}=\Delta p_{dh}=\Delta p$, so that the steady-state momentum equations are

$$\alpha_{\mathbf{a}}Q^n_{\mathbf{a}}=\alpha_{\mathbf{b}}Q^n_{\mathbf{b}}=\alpha_{\mathbf{c}}Q^n_{\mathbf{c}}=\alpha_d Q^n_d=\Delta p_t-\alpha_e Q^n_e=\Delta p \tag{3}$$

where Δp_t is the pressure increase across the pump, assumed to be constant with respect to the flow rate through it. The continuity equation is

$$Q_e-Q_{\mathbf{a}}-Q_{\mathbf{b}}-Q_{\mathbf{c}}-Q_d=0 \tag{4}$$

When $\alpha_{\mathbf{a}}$ undergoes a small change $\delta\alpha_{\mathbf{a}}$, flow rates and pressure will also change. Assuming that the loss coefficients in the responding loops are constant, we can write the linearized variance equations as

$$\begin{pmatrix} n\alpha_{\mathbf{a}}Q^{n-1}_{\mathbf{a},\text{set}} & 0 & 0 & 0 & 0 & -1 \\ 0 & n\alpha_{\mathbf{b}}Q^{n-1}_{\mathbf{b},\text{set}} & 0 & 0 & 0 & -1 \\ 0 & 0 & n\alpha_{\mathbf{c}}Q^{n-1}_{\mathbf{c},\text{set}} & 0 & 0 & -1 \\ 0 & 0 & 0 & n\alpha_d Q^{n-1}_{d,\text{set}} & 0 & -1 \\ 0 & 0 & 0 & 0 & -n\alpha_e Q^{n-1}_{e,\text{set}} & -1 \\ 1 & 1 & 1 & 1 & -1 & 0 \end{pmatrix} \times \begin{pmatrix} \delta Q_{\mathbf{a}} \\ \delta Q_{\mathbf{b}} \\ \delta Q_{\mathbf{c}} \\ \delta Q_d \\ \delta Q_e \\ \delta\Delta p \end{pmatrix} = \begin{pmatrix} -Q^n_{\mathbf{a},\text{set}} \\ 0 \\ 0 \\ 0 \\ 0 \\ 0 \end{pmatrix} \delta\alpha_{\mathbf{a}} \tag{5}$$

For our experiments, the three secondary loops are initially set to be identical so that $Q_{\mathbf{a},\text{set}}=Q_{\mathbf{b},\text{set}}=Q_{\mathbf{c},\text{set}}=Q^c_{\text{set}}$ and $\alpha_{\mathbf{a}}=\alpha_{\mathbf{b}}=\alpha_{\mathbf{c}}$. Writing $\delta(\cdot)=(\cdot)-(\cdot)_{\text{set}}$, we can get

$$\frac{Q_{\mathbf{b}}-Q_{\mathbf{b},\text{set}}}{Q_{\mathbf{b},\text{set}}}=\frac{Q_{\mathbf{c}}-Q_{\mathbf{c},\text{set}}}{Q_{\mathbf{c},\text{set}}}=\frac{Q_d-Q_{d,\text{set}}}{Q_{d,\text{set}}}=-\frac{1}{S}\frac{Q_{\mathbf{a}}-Q_{\mathbf{a},\text{set}}}{Q_{\mathbf{a},\text{set}}} \tag{6}$$

where

$$S=\frac{Q_{e,\text{set}}}{Q_{\mathbf{a},\text{set}}}\frac{\Delta p_t}{\Delta p_t-\Delta p_{\text{set}}}-1 \tag{7}$$

$Q_{\mathbf{a},\text{set}}$, $Q_{e,\text{set}}$, Δp_t, and Δp_{set} can be viewed as the operating parameters which are initially given. With these parameters, the change of the flow rates in the responding loops upon perturbation in the actuating loop can be determined. S defines the slope of the rela-

Table 2 Symbols used in graphs of steady-state response

Symbols	Measurement in loop	Actuation in loop	Symbols	Measurement in loop	Actuation in loop	Setting (ml/s)
△	**a**	**a**	■	**a**	**b**	63
◇	**b**	**a**	◆	**b**	**b**	63
▽	**c**	**a**	▼	**c**	**b**	63
△	**a**	**a**	▲	**a**	**b**	127
+	**b**	**a**	×	**b**	**b**	127
∘	**c**	**a**	●	**c**	**b**	127
▷	**a**	**a**	▶	**a**	**b**	189
*	**b**	**a**	⋆	**b**	**b**	189
◁	**c**	**a**	◀	**c**	**b**	189

Line	Flow rate (ml/s)	Actuating loop
Continuous	189	**a**
Dashed	127	**a**
Dotted	63	**a**
Thick continuous	189	**b**
Thick dashed	127	**b**
Thick dotted	63	**b**

tive changes.

In the same manner, we can get the relative change of the pressure difference as

$$\frac{\Delta p - \Delta p_{\text{set}}}{\Delta p_{\text{set}}} = -\frac{n}{S}\frac{Q_{\mathbf{a}} - Q_{\mathbf{a},\text{set}}}{Q_{\mathbf{a},\text{set}}} \tag{8}$$

and the primary flow rate as

$$\frac{Q_e - Q_{e,\text{set}}}{Q_{e,\text{set}}} = \frac{1}{S}\frac{\Delta p_{\text{set}}}{\Delta p_t - \Delta p_{\text{set}}}\frac{Q_{\mathbf{a}} - Q_{\mathbf{a},\text{set}}}{Q_{\mathbf{a},\text{set}}} \tag{9}$$

The theoretical predictions using Eqs. (6) and (8) with $n=2$ are also shown in Figs. 6 and 7, respectively, where the symbols represent the experimental data and lines represent the modeling results.

The experimental results can be physically explained in the following way. Closing the valve in the actuating loop results in an increase of the flow resistance in that loop and, as a result, an increase of the total resistance in the network and, consequently, a decrease of the total flow rate due to the constant Δp_t. Therefore, the pressure difference decreases on the main loop but increases on the secondary loops. Accordingly, the flow rate in the actuating loop decreases but increases in the responding loops since the flow resistances in those loops are unchanged. Since $S>0$, the one-dimensional model results, Eq. (6), show a similar behavior. In addition, $S>1$ means that the increase in magnitude of the flow rates in the responding loops is always smaller than that in the actuating loop.

Once the operating condition is given, the slopes of the relative change curves are fixed and the response is almost linear. It can be pointed out that the greater the value of Q^c_{set}, the smaller the total resistance in the network and, consequently, there is an increase of pressure difference along the main loop but a decrease along the secondary loops. This combination results in a decrease of S and a higher relative change. From Eqs. (6) and (8), the relative change of the pressure difference is n-times larger than that of the flow rate. For fully turbulent flow, $n=2$ and the relative change of the pressure difference is almost twice that of the flow rate.

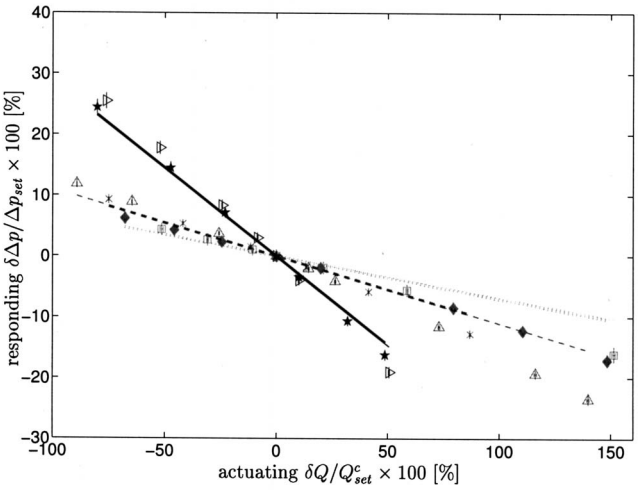

Fig. 6 Change of pressure difference versus change of flow rate in an actuating loop

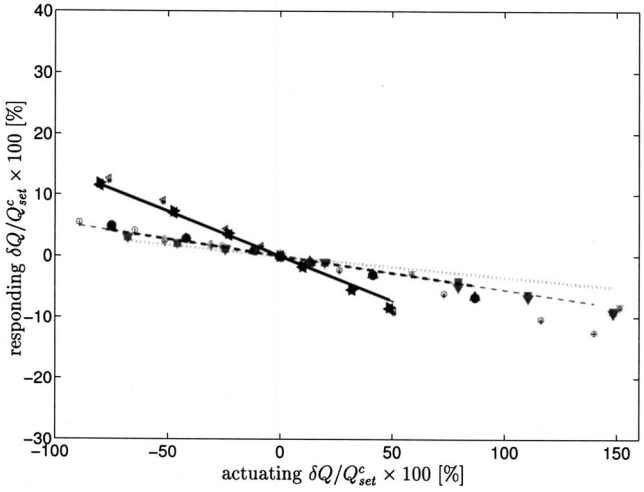

Fig. 7 Change of flow rate in responding loops versus change of flow rate in an actuating loop

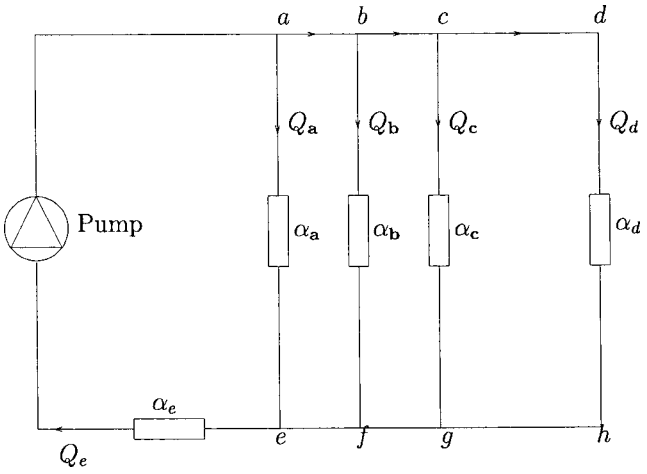

Fig. 8 Schematic of simplified loop

5 Steady-State Thermal Response

In addition to the hydrodynamic interaction between secondaries, the thermal interaction is also important. In this section we analyze the response of the temperature distributions and the heat rates. The symbols used in the graphs are the same as shown in Table 2.

5.1 Experiment. The heat rate at the heat exchangers, q, is determined from

$$q = \rho Q c_p \Delta T \tag{10}$$

where c_p is the specific heat, and $\Delta T = |T_i - T_o|$ is the magnitude of the temperature change of the fluid as it passes through the device. The heat rates on the heating and cooling side are different due to some losses to room air. Table 4 shows the range of the ratio of the heat rate in the cooling loop, q^c, compared to that in the heating loop, q^h, measured in each of the three secondaries. About 10% of the heat is lost to the room, being a little higher for lower flow rates due to higher temperatures. We will ignore these losses and consider only the heat rate at the cooling side of the heat exchangers.

The change in heat rate is affected by two factors: change in flow rate and change in temperature difference. Flow rate changes, considered in the previous section, have been seen to be linear over a wide range of valve actuation. Figure 9 shows the temperature change in the actuating loop. The behavior over the same range is more quadratic, and the value of Q^c_{set} does not seem to make much difference. Figure 10 shows the temperature change in the responding loops. The temperature change is much smaller and is dependent on Q^c_{set}. For $Q^c_{\text{set}}=63$ ml/s, a decrease of flow rate in the actuating loop results in a decrease of the total flow rate causing a decrease of the inlet flow temperature and an increase of the flow rates in the responding loops; therefore, the temperature differences in the responding loops increase. The larger the initial value of the flow rate, the greater is the flow rate increase in the responding loops with the same relative change of the flow in the actuating loop. The heat rate, however, is almost independent of the flow rate setting. Therefore, at $Q^c_{\text{set}}=127$ ml/s, the same trend of the change of the temperature difference is observed but the relative change is reduced. At $Q^c_{\text{set}}=189$ ml/s, the relative change of the flow rate continuously increases while the relative change of the heat rate is almost constant, so that the change of temperature difference shows a trend opposite to that for the other two Q^c_{set} values. It is reasonable to expect that there is a flow rate between $Q^c_{\text{set}}=127$ ml/s and $Q^c_{\text{set}}=189$ ml/s at which the temperature difference is constant while the flow rate is changing.

Table 4 Ratio of heat rates in cooling and heating sides of the heat exchangers

	$Q^c_{\text{set}}=63$ ml/s	$Q^c_{\text{set}}=127$ ml/s	$Q^c_{\text{set}}=189$ ml/s
$q^c_{\mathbf{a}}/q^h_{\mathbf{a}}$	0.794–0.869	0.826–0.883	0.841–0.866
$q^c_{\mathbf{b}}/q^h_{\mathbf{b}}$	0.934–0.948	0.954–0.965	0.943–0.954
$q^c_{\mathbf{c}}/q^h_{\mathbf{c}}$	0.913–0.957	0.923–0.955	0.927–0.934

In the actuating loop, the reduced flow rate causes a rapid decrease of the heat transfer coefficient and, therefore, a decrease of the heat transfer rate as shown in Fig. 11. The nonlinearity of the thermal response over the same range is obvious in comparison to the hydrodynamic response. Figure 12 shows the change in the heat rate in the responding loops. A decrease of flow rate in the actuating loop causes an increase of heat rate in the responding loops. There is a decrease of the total flow rate in the main loop causing a decrease of the outlet temperature of the cooling water when running through the compact plate heat exchanger HX_m and, as a result, the decrease of the inlet temperature in the cooling side of heat exchangers in the secondary loops. The decrease of the flow temperature, combined with the increase of the flow rates in the responding loops and therefore the increase of the heat transfer coefficient, results in the increase of the heat rates in the cooling sides of heat exchangers. The responses of the heat rates are contrary to the hydrodynamic responses in that at larger initial setting, the relative changes of the heat rates are smaller. However, it is noticed that there is little difference among the responses for different Q^c_{set}.

5.2 Model. The governing equations for the heat exchanger in loop **a** are

$$q_{\mathbf{a}} = U_{\mathbf{a}} A_{\mathbf{a}} F_{\mathbf{a}} [(T^h_i - T^c_{\mathbf{a},o}) - (T^h_{\mathbf{a},o} - T^c_i)] \left[\ln \frac{T^h_i - T^c_{\mathbf{a},o}}{T^h_{\mathbf{a},o} - T^c_i} \right]^{-1} \tag{11}$$

$$= \rho Q^h C_p (T^h_i - T^h_{\mathbf{a},o}) \tag{12}$$

$$= \rho Q_{\mathbf{a}} C_p (T^c_{\mathbf{a},o} - T^c_i) \tag{13}$$

where T^h_i is the heating water inlet temperature and T^c_i is the cooling water inlet temperature. U is the overall heat transfer coefficient, A is the area, and F is the correction factor that is used for heat exchangers. After some manipulation, we get

$$q_{\mathbf{a}} = \frac{\rho C_p (T^h_i - T^c_i) \left[\exp\left\{ \frac{U_{\mathbf{a}} A_{\mathbf{a}} F_{\mathbf{a}}}{\rho C_p} \left(\frac{1}{Q^h} - \frac{1}{Q_{\mathbf{a}}} \right) \right\} - 1 \right]}{\exp\left\{ \frac{U_{\mathbf{a}} A_{\mathbf{a}} F_{\mathbf{a}}}{\rho C_p} \left(\frac{1}{Q^h} - \frac{1}{Q_{\mathbf{a}}} \right) \right\} \frac{1}{Q^h} - \frac{1}{Q_{\mathbf{a}}}} \tag{14}$$

Similar expressions can be written for $q_{\mathbf{b}}$ and $q_{\mathbf{c}}$.

In the primary loop

Table 3 Pressure drops for different flow rates

	$Q^c_{\text{set}}=63$ ml/s	$Q^c_{\text{set}}=127$ ml/s	$Q^c_{\text{set}}=189$ ml/s
$(1-\Delta p_{bf}/\Delta p_{ae})\times 100$	2.53–2.56	1.78–2.32	2.21–2.31
$(1-\Delta p_{cg}/\Delta p_{ae})\times 100$	6.15–7.54	4.10–6.80	4.61–7.39

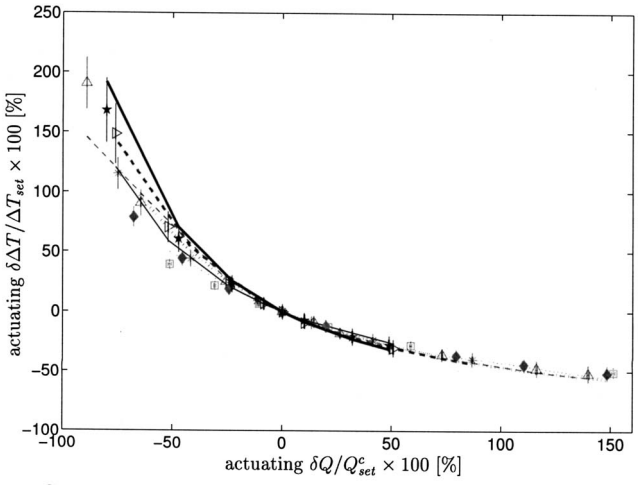

Fig. 9 Change of temperature difference in an actuating loop versus that of the flow rate

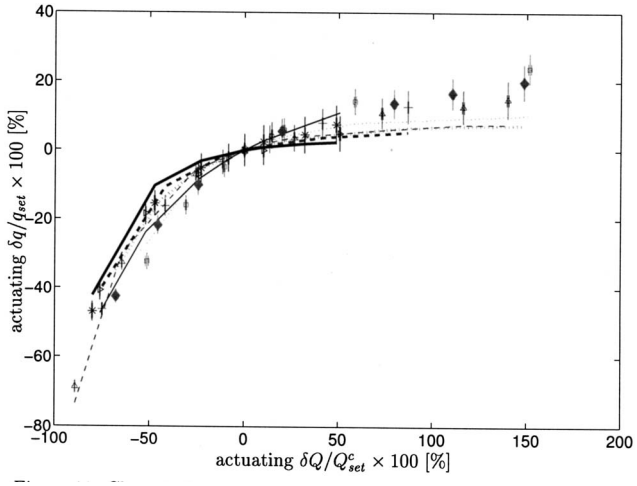

Fig. 11 Change of heat rate in an actuating loop versus that of the flow rate

$$q_e = \rho Q_e c_p (T_e - T_i^c) \tag{15}$$

$$= \frac{\rho c_p (T_e - T_i^{\mathrm{ch}}) \left[\exp\left\{ \frac{U_e A_e F_e}{\rho c_p} \left(\frac{1}{Q_e} - \frac{1}{Q^{\mathrm{ch}}} \right) \right\} - 1 \right]}{\exp\left\{ \frac{U_e A_e F_e}{\rho c_p} \left(\frac{1}{Q_e} - \frac{1}{Q^{\mathrm{ch}}} \right) \right\} \frac{1}{Q_e} - \frac{1}{Q^{\mathrm{ch}}}} \tag{16}$$

where T_e is the inlet cooling water temperature of the primary heat exchanger, T_i^{ch} is the chiller inlet temperature, and Q^{ch} is the chiller volumetric flow rate. From this and the energy balance

$$q_e = q_{\mathbf{a}} + q_{\mathbf{b}} + q_{\mathbf{c}} \tag{17}$$

we can find

$$T_i^c = \frac{(r_{\mathbf{a}} + r_{\mathbf{b}} + r_{\mathbf{c}}) T_i^h + r_e T_i^{\mathrm{ch}}}{r_{\mathbf{a}} + r_{\mathbf{b}} + r_{\mathbf{c}} + r_e} \tag{18}$$

The temperature difference and heat rate in the heat exchanger are then

$$\Delta T_j^c = \frac{r_j}{\rho Q_j} \frac{r_e}{r_{\mathbf{a}} + r_{\mathbf{b}} + r_{\mathbf{c}} + r_e} (T_i^h - T_i^{\mathrm{ch}}) \tag{19}$$

$$q_j = r_j \frac{r_e}{r_{\mathbf{a}} + r_{\mathbf{b}} + r_{\mathbf{c}} + r_e} C_p (T_i^h - T_i^{\mathrm{ch}}) \quad j = \mathbf{a}, \mathbf{b}, \mathbf{c} \tag{20}$$

where

$$r_j = \frac{\exp_j(\cdot) - 1}{\exp_j(\cdot) \frac{1}{\rho Q^h} - \frac{1}{\rho Q_j}} \quad j = \mathbf{a}, \mathbf{b}, \mathbf{c} \tag{21}$$

$$r_e = \frac{\exp_e(\cdot) - 1}{\frac{1}{\rho Q_e} - \frac{1}{\rho Q^{\mathrm{ch}}}} \tag{22}$$

$$\exp_j(\cdot) = \exp\left[\frac{U_j A_j F_j}{\rho C_p} \left(\frac{1}{Q^h} - \frac{1}{Q_j} \right) \right] \quad j = \mathbf{a}, \mathbf{b}, \mathbf{c} \tag{23}$$

$$\exp_e(\cdot) = \exp\left[\frac{U_e A_e F_e}{\rho C_p} \left(\frac{1}{Q_e} - \frac{1}{Q^{\mathrm{ch}}} \right) \right] \tag{24}$$

Q^h, T_i^h, Q^{ch}, and T_i^{ch} are parameters that are fixed during the experiments. The correction factor F is available in chart form [16]. Assuming that wall thermal resistance and fouling are neg-

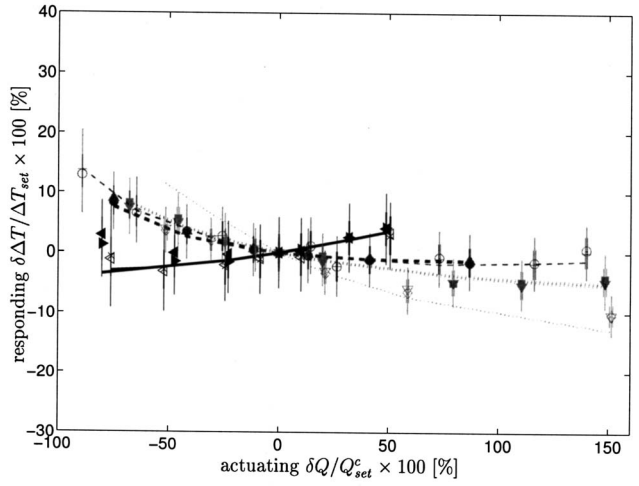

Fig. 10 Change of temperature difference in responding loops versus that of the flow rate in actuating loop

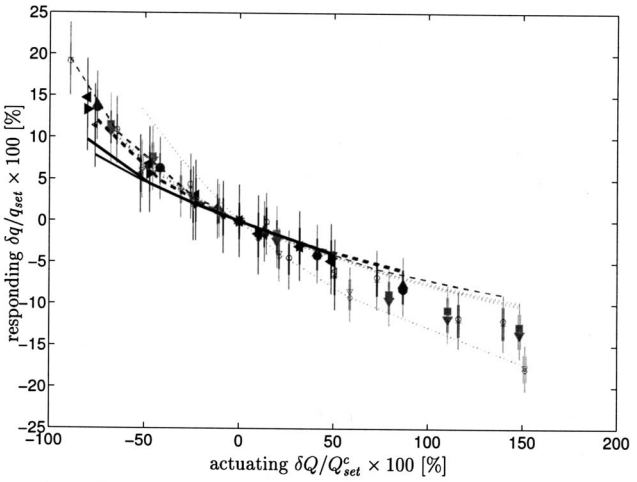

Fig. 12 Change of heat rate in responding loops versus change of flow rate in an actuating loop

ligible, and also assuming equal surface areas on both sides, the overall heat transfer coefficient can be written as

$$\frac{1}{U_i} = \frac{1}{h_i^h} + \frac{1}{h_i^c} \quad \text{for } i = \mathbf{a}, \mathbf{b}, \mathbf{c}, e \tag{25}$$

For shell-tube heat exchangers, the tube-side heat transfer coefficient (which is the heating side) h^h is given by [17]

$$\frac{h^h d_i}{k^h} = 0.03(\mathrm{Re}^h)^{0.79}(\mathrm{Pr}^h)^{0.3} \quad 1200 < \mathrm{Re}^h < 5.3 \times 10^4 \tag{26}$$

The Reynolds number and the Prandtl number are defined as $\mathrm{Re}^h = \rho u^h d_i / \mu^h$ and $\mathrm{Pr}^h = c_p \mu^h / k^h$, respectively, and u is the flow velocity inside tubes, d_i is the tube inner diameter, μ is the viscosity, and k is the thermal conductivity. The shell-side heat transfer correlation suggested by [18] is

$$\frac{h^c d_o}{k^c} = 0.2(\mathrm{Re}^c)^{0.6}(\mathrm{Pr}^c)^{0.4} \tag{27}$$

where $\mathrm{Re}^c = \rho Q d_o / A_s \mu^c$ and $\mathrm{Pr}^c = c_p \mu^c / k^c$, respectively, and d_o is tube outside diameter and A_s is the cross-flow area of the shell diameter.

The heat transfer coefficients on heating and cooling sides of the compact plate heat exchanger are [16]

$$\frac{h d_e}{k} = C_h(\mathrm{Re}^{\mathrm{ch}})^m \mathrm{Pr}^{1/3}\left(\frac{\mu_f}{\mu_w}\right)^{0.17} \tag{28}$$

where μ_f and μ_w are the dynamic viscosities of water at the bulk and wall temperature, respectively. Also, $\mathrm{Re}^{\mathrm{ch}} = \rho Q d_e / N_c A_x \mu^{\mathrm{ch}}$, and the equivalent diameter is $d_e = 4A_x / P_w$; A_x is the channel flow area, and P_w is the wetted perimeter determined by the geometry of the heat exchanger. The values of C_h and m are available [16,19].

For loop **a**, for example, $Q_{\mathbf{a}}$ and Q_e can be obtained from Eqs. (6) and (9) based on the mathematical model. $\Delta T_{\mathbf{a}}^c$ and $q_{\mathbf{a}}$ can be calculated from Eqs. (19) and (20). Similar expressions may be found for loops **b** and **c**. All the properties are calculated based on the inlet and outlet mean temperature through numerical iterations.

It can be noticed that a common part of the expressions for temperature differences and heat rates for loops **a**, **b**, and **c** is $(T_i^h - T_i^{\mathrm{ch}})\ R$, where

$$R = \frac{r_e}{r_{\mathbf{a}} + r_{\mathbf{b}} + r_{\mathbf{c}} + r_e} \tag{29}$$

which involves the four heat exchangers in the network and represents the thermal interaction. This term contributes equally to each secondary loop since they are connected in parallel with the primary and have the same inlet cooling-water temperature on the cooling side.

The results are shown in Figs. 9–12 where again the symbols represent the experimental data and lines represent the results of the model. The changes of the temperature differences and flow rates can be explained by Eqs. (19) and (20). Taking actuation in loop **a** as an example, $r_{\mathbf{a}}R$ increases with $Q_{\mathbf{a}}$. The increasing rate of $r_{\mathbf{a}}R$, however, is slower than that of $Q_{\mathbf{a}}$. Therefore, on the actuating loop, the temperature difference decreases while the heat rate increases with $Q_{\mathbf{a}}$.

In the responding loops, $r_{\mathbf{b}}R$ and $r_{\mathbf{c}}R$ decrease while $Q_{\mathbf{a}}$ increases. Thus the heat rate decreases. It is shown that the flow rates $Q_{\mathbf{b}}$ and $Q_{\mathbf{c}}$ decrease while $Q_{\mathbf{a}}$ increases. The relative change of the flow rate is smaller than that of $r_{\mathbf{b}}R$ or $r_{\mathbf{c}}R$ at $Q_{\mathrm{set}}^c = 63$ ml/s. Therefore, the temperature difference decreases while $Q_{\mathbf{a}}$ increases. At $Q_{\mathrm{set}}^c = 127$ ml/s, the same trend of the change of the temperature difference is observed but the relative change is reduced. At $Q_{\mathrm{set}}^c = 189$ ml/s, the relative change of the flow rate is a little bit faster than that of the heat rate. Therefore, the temperature difference increases while $Q_{\mathbf{a}}$ increases.

6 Conclusions

It is observed that the response time of the temperature is an order of magnitude higher than that of the flow rate, and that of the pressure difference is an order of magnitude lower. As a consequence of this, it is reasonable in complex network studies to assume that pressure changes take place instantaneously, while the flow rates and temperatures respond more slowly.

The present study investigated the interaction between the secondary loops in a thermal-hydraulic network. The network is small enough relative to flow rates, heat transfer rates, pipe length, and total thermal capacitance, so that little effect was found of the distance between interacting loops. In a real network, the pipe length can be very large and, therefore, the pressure difference between secondary loops cannot be neglected.

Interactions between secondary loops depend on initial flow rates. The higher it is, the stronger the hydrodynamic interaction. Both flow rates and pressure differences show a linear response. Thermal interaction is a result of hydrodynamic interaction; it is nonlinear and also different for different loops and initial flow rates.

The net result is that, in the present case at least, each secondary cannot be treated as isolated from the others. There is interaction between them that can be significant for some initial flow rates. The present work quantifies the interaction, so that in applications it may be a priori determined whether it is negligible or not for the purpose at hand.

Acknowledgment

We acknowledge the support provided to W. C. and W. F. by the late Mr. D.K. Dorini of BRDG-TNDR and the Hydronics Laboratory.

Nomenclature

- $\mathbf{a}, \mathbf{b}, \mathbf{c}$ = secondary loops
- A = heat transfer area (m^2)
- A_s = cross flow area of shell diameter (m^2)
- A_x = channel flow area (m^2)
- c_p = specific heat at constant pressure (J/kg K)
- C_h = parameter used in Eq. (28)
- d_i = tube inner diameter (m)
- d_o = tube outer diameter (m)
- d_e = equivalent diameter (m)
- D = pipe diameter (m)
- F = heat exchanger correction factor
- h = convective heat transfer coefficient ($\mathrm{W/m^2\ s}$)
- k = thermal conductivity (W/m K)
- L = pipe length (m)
- m = exponent defined in Eq. (28)
- n = exponent used in Eq. (1)
- N_c = number of channels per pass
- Pr = Prandtl number
- P_w = wetted perimeter (m)
- Δp = pressure difference (Pa)
- Δp_t = pressure difference generated by pump (Pa)
- Δp_{ij} = pressure difference between points i and j (Pa)
- q = heat rate (W)
- Q = volumetric flow rate ($\mathrm{m^3/s}$)
- r = parameter defined in Eqs. (21) and (22) (kg/s)
- R = parameter defined in Eq. (29)
- Re = Reynolds number
- S = parameter defined in Eq. (7)
- t = time (s)
- T = temperature (°C)
- ΔT = temperature difference (°C)
- u = velocity (m/s)
- U = overall heat transfer coefficient ($\mathrm{W/m^2\ s}$)

Greek symbols

α = loss coefficient ($kg/m^{3n+1}\ s^{2-n}$)
β = parameter defined by Eq. (2) (kg/m^4)
μ = dynamic viscosity (kg/m s)
ρ = density (kg/m^3)

Subscripts

a, **b**, **c** = secondary loops
a-h = nodes
f = fluid
i = inlet
o = outlet
set = initial setting
w = wall

Superscripts

c = cooling side
ch = chilling side
h = heating side

References

[1] Kirsner, W., 1995, "Chilled Water Distribution Problems," Heat./Piping/Air Cond., **67**(2), pp. 51–59.
[2] Weber, J. A., 1989, "Solving the Piping Problems in Chilled Water Systems," Plant Eng., **43**(13), pp. 94–97.
[3] Rishel, J. B., 1994, "Piping Chillers to Variable Volume Chilled Water Systems," ASHRAE J., **36**(7), pp. 43–45.
[4] Fiorino, D. P., 1999, "Achieving High Chilled-Water Delta *Ts*," ASHRAE J., **41**(11), pp. 24–30.
[5] Kirsner, W., 1995, "Troubleshooting Chilled-Water Distribution Problems at NASA Johnson Space Center," Heat./Piping/Air Cond., **67**(2), pp. 51–59.
[6] Kirsner, W., 1996, "The Demise of the Primary-Secondary Pumping Paradigm for Chilled Water Plant Design," Heat./Piping/Air Cond., **68**(11), pp. 73–78.
[7] Larsen, H. V., Pálsson, H., Bøhm, B., and Ravnd, H. F., 2002, "Aggregated Dynamic Simulation Model of District Heating Networks," Energy Convers. Manage., **43**(8), pp. 995–1019.
[8] Franco, W., Sen, M., Yang, K. T., and McClain, R. L., 2004, "Dynamics of Thermal-Hydraulic Network Control Strategies," Exp. Heat Transfer, **17**(3), pp. 161–179.
[9] Fu, L., Jiang, Y., Yuan, W., and Qin, X., 2001, "Influence of Supply and Return Water Temperatures on the Energy Consumption of a District Cooling System," Appl. Therm. Eng., **21**(4), pp. 511–521.
[10] Bajsić, I., and Bobič, M., 2006, "Modelling and Experimental Validation of a Hot Water Supply Substation," Energy Build., **38**(4), pp. 327–333.
[11] Franco, W., Sen, M., Yang, K. T., and McClain, R. L., 2001, "Modeling and Control of a Thermal-Hydraulic Network," Proceedings of the ASME NHTC'01, 35th National Heat Transfer Conference, NHT2001-20156.
[12] Bojic, M., and Trifunovic, N., 1999, "Linear Programming Optimization of Heat Distribution in a District-Heating System by Valve Adjustments and Substation Retrofit," Build. Environ., **35**(2), pp. 151–159.
[13] Kim, J.-K., and Smith, R., 2003, "Automated Retrofit Design of Cooling-Water Systems," AIChE J., **49**(7), pp. 1712–1730.
[14] Choy, F. K., Brau, M. J., and Wang, H. S., 1996, "Transient Pressure Analysis in Piping Networks Due to Valve Closing and Outlet Pressure Pulsation," J. Pressure Vessel Technol., **118**(3), pp. 315–325.
[15] Orfanidis, S. J., 1996, *Introduction to Signal Processing*, Prentice-Hall, NJ.
[16] Kraus, A. D., 2003, "Heat Exchangers," in *Heat Transfer Handbook*, A. Bejan and A. D. Kraus, eds., Wiley, Hoboken, NJ.
[17] Zhao, X., 1995, "Performance of a Single-Row Heat Exchanger at Low In-Tube Flow Rates," M.S. thesis, Department of Aerospace and Mechanical Engineering, University of Notre Dame, Notre Dame, Indiana.
[18] Taborek, J., 1991, "Industrial Heat Exchanger Design Practice," in *Boilers, Evaporators, and Condensers*, S. Kakaç, ed., Wiley, New York.
[19] Saunders, E. A. D., 1988, *Heat Exchangers-Selection, Design, and Construction*, Wiley, New York.